



JOURNAL OF  
SYNCHROTRON  
RADIATION

**Volume 29 (2022)**

**Supporting information for article:**

**From EXAFS of reference compounds to U(VI) speciation in  
contaminated environments**

**Anna Krot, Irina Vlasova, Alexander Trigub, Alexey Averin, Vasily Yapaskurt  
and Stepan Kalmykov**

## S1. Powder X-ray diffraction

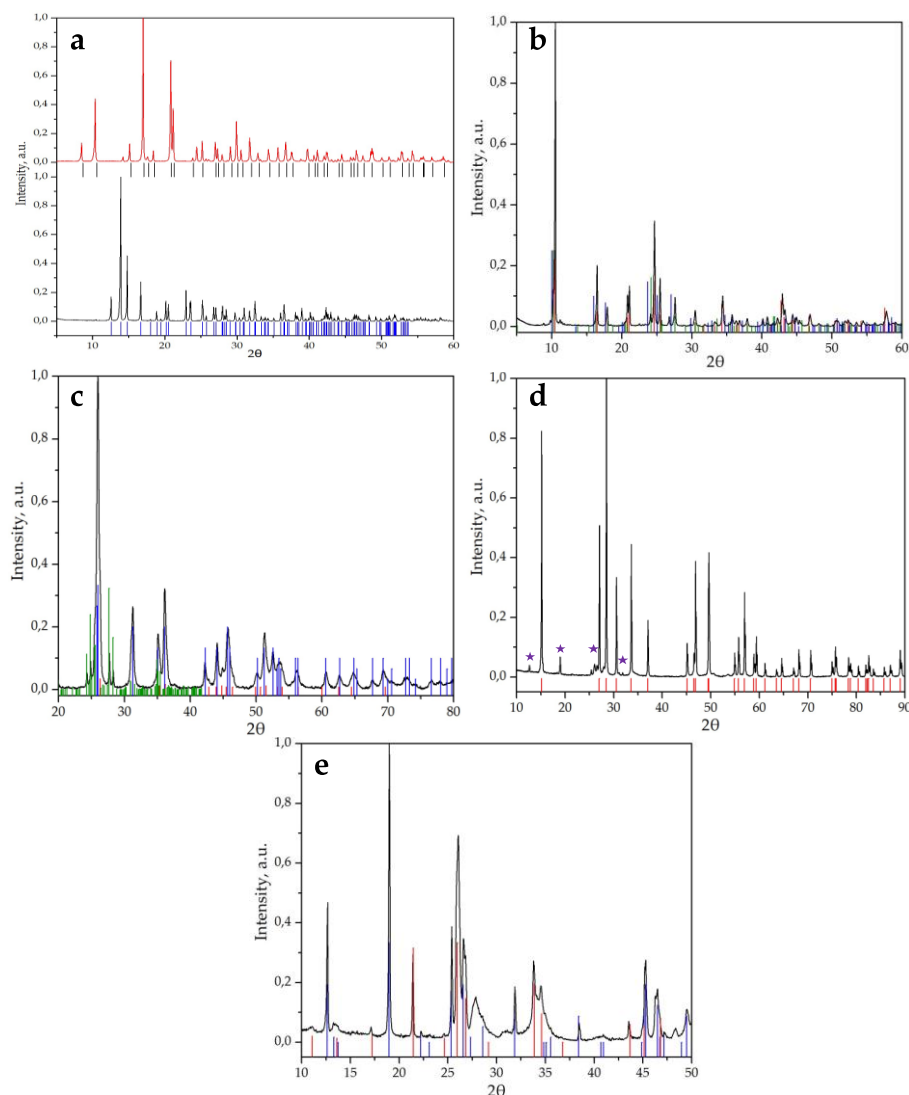


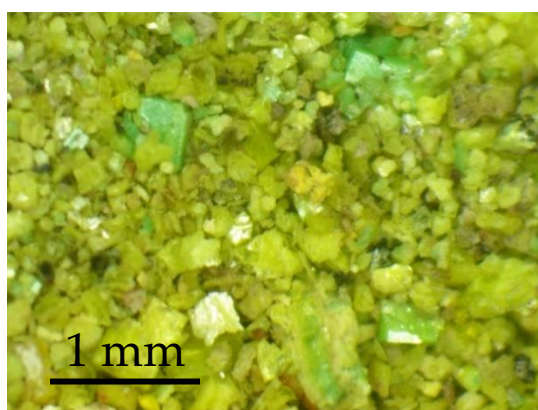
**Figure S1** Powder X-ray diffraction of: **(a)** synthesized  $(\text{UO}_2)_3(\text{PO}_4)_2 \cdot 4\text{H}_2\text{O}$  (red) and  $(\text{NH}_4)_4\text{UO}_2(\text{CO}_3)_3$  (black). Reflections are in a good agreement with PDF 00-037-0369 and PDF 01-073-0040, respectively; **(b)** mixture of natural phosphate minerals. Red patterns corresponds to metaautunite  $\text{Ca}(\text{UO}_2)_2(\text{PO}_4)_2 \cdot 3\text{H}_2\text{O}$  (PDF 00-039-1351), green to torbernite  $\text{Cu}(\text{UO}_2)_2(\text{PO}_4)_2 \cdot 8\text{H}_2\text{O}$  (PDF 00-036-0406) and blue to metazeunerite  $\text{Cu}(\text{UO}_2)_2(\text{AsO}_4)_2 \cdot 8\text{H}_2\text{O}$  (PDF 01-077-0124); **(c)** synthesized uranium oxyhydroxide. Three phases were identified: metaschoepite  $\text{UO}_3 \cdot 2\text{H}_2\text{O}$  (PDF 01-070-4765) – green pattern, and dehydrated phases  $\text{UO}_3 \cdot \text{H}_2\text{O}$  (PDF 00-013-0242) – red pattern,  $\text{UO}_3 \cdot 0.8\text{H}_2\text{O}$  (PDF 00-010-0309) – blue pattern; **(d)**  $\text{CaUO}_4$ . Red patterns correspond to  $\text{CaUO}_4$  structure (PDF 01-085-0577), purple stars indicate reflections of impurity  $\text{CaU}_2\text{O}_7$  phase (PDF 00-044-0581); **(e)**  $\text{CaU}_2\text{O}_7$ . Blue patterns correspond to  $\text{CaU}_2\text{O}_7$  phase (PDF 00-044-0581), red – to impurity of uranate of different composition,  $\text{CaU}_5\text{O}_{15.4}$  (PDF 00-022-0817).

**S2. SEM-EDX****Table S1** Standards for EDX quantitative analysis.

Element	P	Ca	As	Cu	Sr	U
series	K	K	K	K	K	M
standard	GaP	Cpx-164905	InAs	Cu	SrF <sub>2</sub>	UO <sub>2</sub>
Sigma, wt%	0.02	0.02	0.02	0.03	0.10	0.20

**Table S2** EDX data on mineral system composition, at.%. “Autunite” represents points, recorded on yellow crystals which consist of Ca-UO<sub>2</sub> phosphate mineral, “Torbernite” – green crystals of Cu-UO<sub>2</sub> mineral. Oxygen calculated by stoichiometry.

Point	All results in atomic %								
	P	As	Ca	Cu	Sr	U	O	U:(P+As)	U:(Ca+Sr)
Torbernite-1	7.94	3.89		5.91		11.69	70.57	1.0	2.0
Torbernite-2	7.83	4.1		5.61		11.76	70.7	1.0	2.1
Torbernite-3	8.25	3.95		5.4		11.62	70.77	1.0	2.2
Torbernite-4	10.37	1.5		5.17		12.03	70.93	1.0	2.3
Autunite-1	11.25	0.7	5.52		0.34	11.61	70.58	1.0	2.0
Autunite-2	10.73	0.83	5.68		0.33	11.88	70.55	1.0	2.0

**Figure S2** Optical image of the mixture of phosphate minerals. Yellow crystals represent Ca-uranyl phosphate, green – Cu-containing phases.

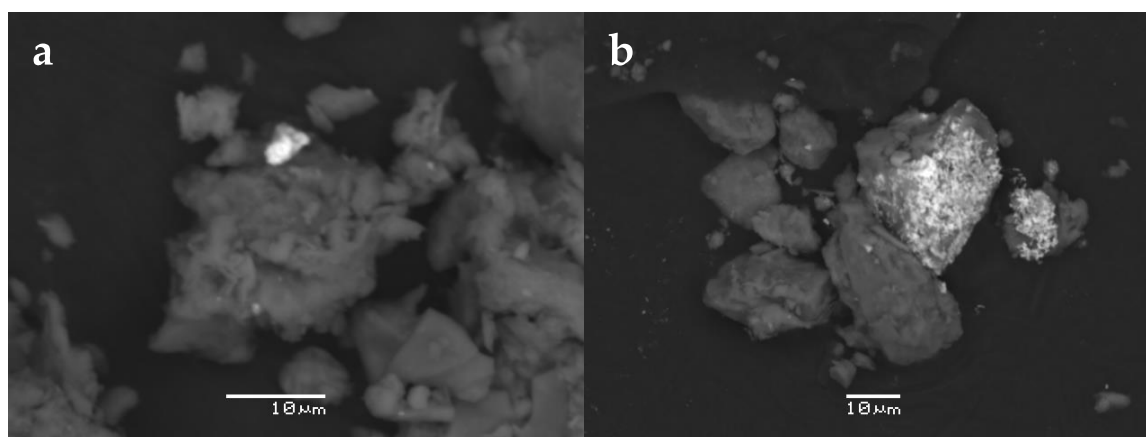


**Figure S3** SEM images of particles (a) and coatings (b) with high U content in the UCS sample.

### S3. Raman spectroscopy

**Table S3** Raman shifts of  $(\text{NH}_4)_4\text{UO}_2(\text{CO}_3)_3$  compared to literature data for similar compounds. Ionic charges are omitted for simplicity.

Compound	$(\text{NH}_4)_4\text{UO}_2(\text{CO}_3)_3$	$\text{Na}_2\text{Ca}(\text{UO}_2)(\text{CO}_3)_3 \cdot x\text{H}_2\text{O}$	$\text{Ca}_2\text{Cu}(\text{UO}_2)(\text{CO}_3)_4 \cdot 6\text{H}_2\text{O}$
$\nu_2 (\text{UO}_2)$	142, 185, 249, 276, 309	164, 182, 224, 242, 272, 284, 299	140, 169, 212, 230, 266
$\nu (\text{U-O}_{\text{eq}})$			
$\delta (\text{U-O}_{\text{eq}})$			
$\nu_4 (\text{CO}_3)$	693, 721, 729	696, 742	731, 756
$\nu_1 (\text{UO}_2)/\nu_2 (\text{CO}_3)$	817	831, 833	826, 834, 840
$\nu_3 (\text{UO}_2)$		(IR)	(IR 897)
$\nu_1 (\text{CO}_3)$	1062	1080, 1092	1074, 1092
$\nu_3 (\text{CO}_3)$	1334, 1408	1370, 1406	1381, 1566
$\text{H}_2\text{O}$		3415, 3510, 3558	3240, 3290, 3383, 3495
Reference	This work	Frost et al. (2004)	Faulques et al. (2018)

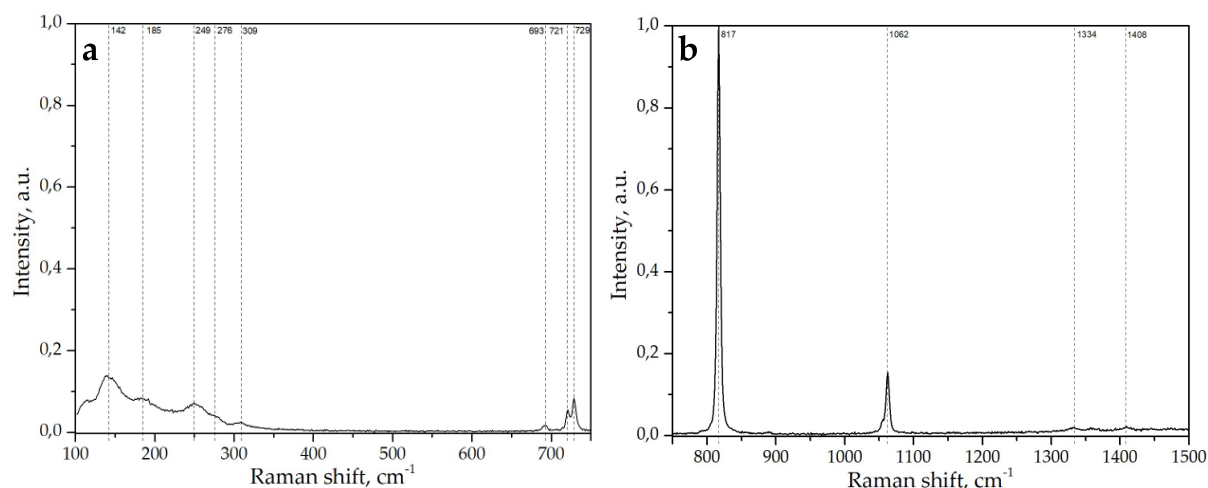


**Figure S4** Raman spectrum of  $(\text{NH}_4)_4\text{UO}_2(\text{CO}_3)_3$ , recorded at 633 nm. (a) 100-750  $\text{cm}^{-1}$  region; (b) 750-1500  $\text{cm}^{-1}$  region.

**Table S4** Raman shifts of  $(\text{UO}_2)_3(\text{PO}_4)_2 \cdot 4\text{H}_2\text{O}$  compared to literature data for similar compounds. Ionic charges are omitted for simplicity.

Compound	$(\text{UO}_2)_3(\text{PO}_4)_2 \cdot 4\text{H}_2\text{O}$	$(\text{UO}_2)_3(\text{PO}_4)_2 \cdot 4\text{H}_2\text{O}$	$(\text{UO}_2)_3(\text{PO}_4)_2 \cdot 4\text{H}_2\text{O}$
v2 ( $\text{UO}_2$ )	182, 208, 219, 230, 246, 289	289	185, 290
v ( $\text{U-O}_{\text{eq}}$ )			
$\delta$ ( $\text{U-O}_{\text{eq}}$ )			
v2 ( $\text{PO}_4$ )	450		450
v4 ( $\text{PO}_4$ )	617		620
v1 ( $\text{UO}_2$ )	846, 867	868	868
v3 ( $\text{UO}_2$ )/v1 ( $\text{PO}_4$ )	923		916
v3 ( $\text{PO}_4$ )	1005, 1031, 1103, 1153	1005, 1033, 1153	1007, 1035, 1115, 1153
$\text{H}_2\text{O}$	3505		
Reference	This work	Armstrong (2009)	Pham-Thi&Colomban (1985)

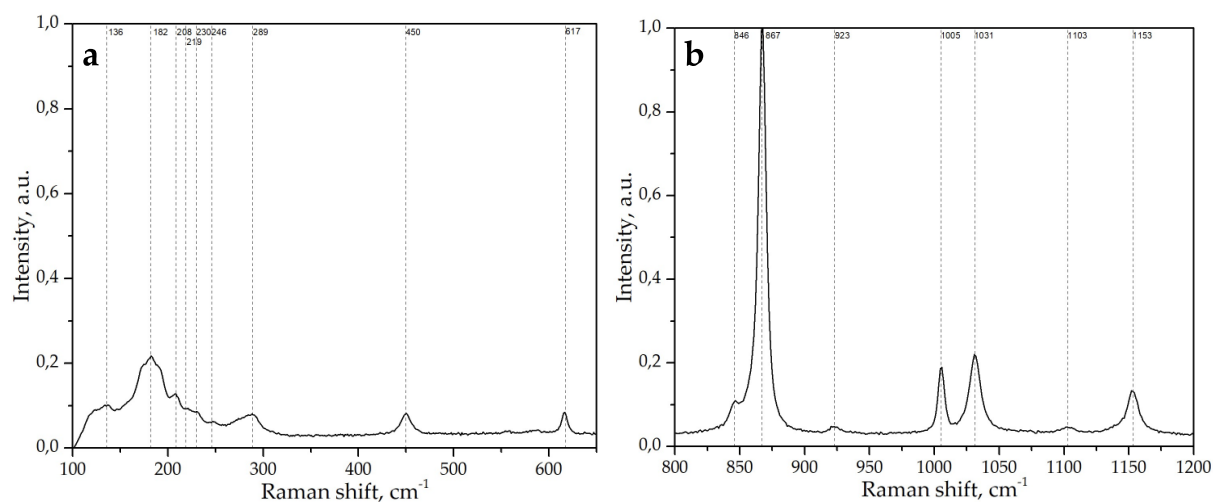


**Figure S5** Raman spectrum of  $(\text{UO}_2)_3(\text{PO}_4)_2 \cdot 4\text{H}_2\text{O}$ , recorded at 633 nm. (a) 100-650  $\text{cm}^{-1}$  region; (b) 800-1200  $\text{cm}^{-1}$  region.

**Table S5** Raman shifts of Cu-phases in the mixture of natural phosphate minerals compared to literature data for Cu-uranyl phosphate and arsenate. Ionic charges are omitted for simplicity.

Compound	Cu-mineral	$\text{Cu}(\text{UO}_2)_2(\text{AsO}_4)_2 \cdot 8\text{H}_2\text{O}$	$\text{Cu}(\text{UO}_2)_2(\text{PO}_4)_2 \cdot 8\text{H}_2\text{O}$
v2 ( $\text{UO}_2$ )	191, 221, 247, 282	218, 240, 276	222, 290
v2 ( $\text{AsO}_4$ )	317	320	
v2 ( $\text{PO}_4$ )	405, 439, 455		399, 406, 439, 464
v4 ( $\text{AsO}_4$ )	455	398, 449	
v1 ( $\text{UO}_2$ )	820, 855	809, 819	808, 826
v3 ( $\text{UO}_2$ )		809, 819	
v1 ( $\text{AsO}_4$ )		810 (v1+ v3)	
v3 ( $\text{AsO}_4$ )	890	888, 910	
v3 ( $\text{PO}_4$ )	976, 989, 1000		957, 988, 995, 1004
Reference	This work	Frost&Weier (2004)	Frost&Weier (2004)

**Table S6** Raman shifts of Ca-phase in the mixture of natural phosphate minerals compared to literature data for Ca-uranyl phosphates. Ionic charges are omitted for simplicity.

Compound	Ca-mineral	$\text{Ca}(\text{UO}_2)_2(\text{PO}_4)_2 \cdot 12\text{H}_2\text{O}$	$\text{Ca}(\text{UO}_2)_2(\text{PO}_4)_2 \cdot 6\text{H}_2\text{O}$
v2 ( $\text{UO}_2$ )	195, 202	222, 291	222, 263
v2 ( $\text{PO}_4$ )		399, 406, 439, 464	387, 453
v4 ( $\text{PO}_4$ )		629	507, 643
v1 ( $\text{UO}_2$ )	796, 818, 836	816, 822, 833	818, 833, 850
v3 ( $\text{UO}_2$ )	860		
v1 ( $\text{PO}_4$ )			
v3 ( $\text{PO}_4$ )	989, 1013, 1027	988, 1007, 1018	989, 1007, 1018, 1033, 1093
Reference	This work	Frost&Weier (2004)	Frost&Weier (2004)

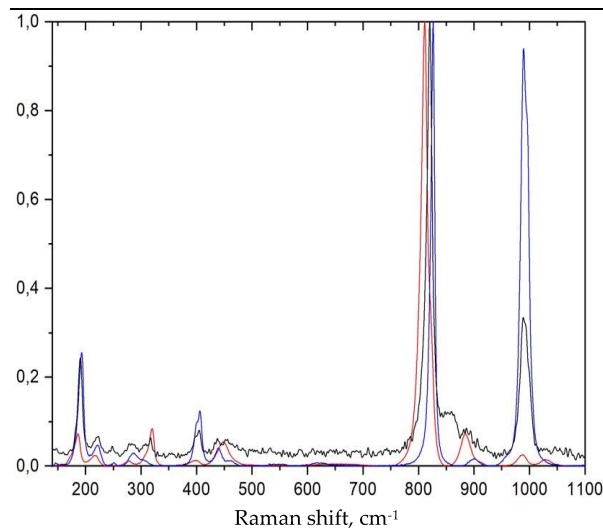


**Figure S6** Comparison of Raman shifts of single-phase metazeunerite  $\text{Cu}(\text{UO}_2)_2(\text{AsO}_4)_2 \cdot 8\text{H}_2\text{O}$  (RRUF ID: R050524) - red, torbernite  $\text{Cu}(\text{UO}_2)_2(\text{PO}_4)_2 \cdot 8\text{H}_2\text{O}$  (RRUF ID: R070509) – blue, and Cu-mineral of the natural mixture - black.

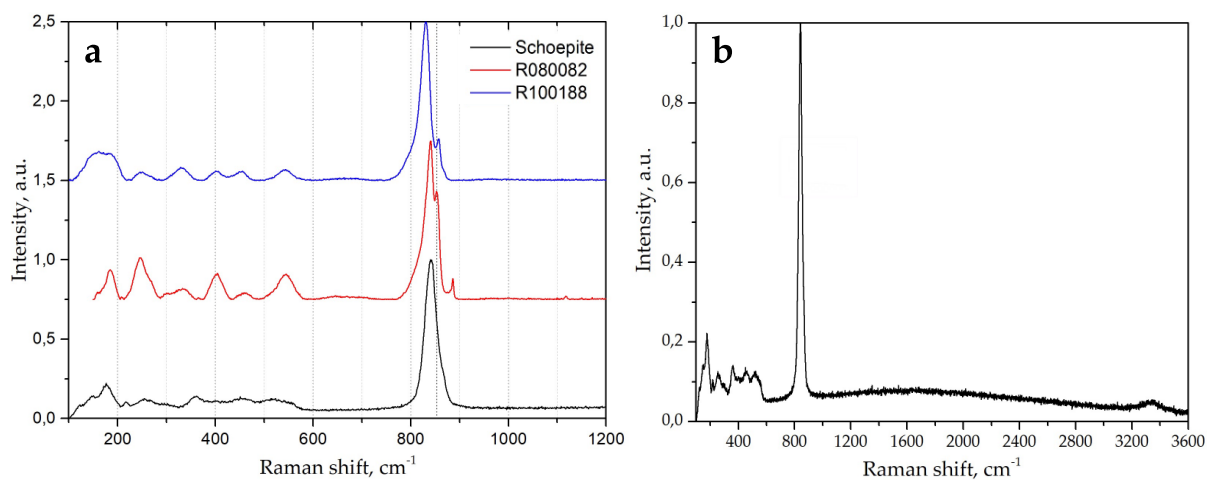


**Figure S7** Raman spectrum of metaschoepite, recorded at 633 nm. (a) Comparison with data from RRUF Database; (b) spectrum in 100-3600  $\text{cm}^{-1}$  region.

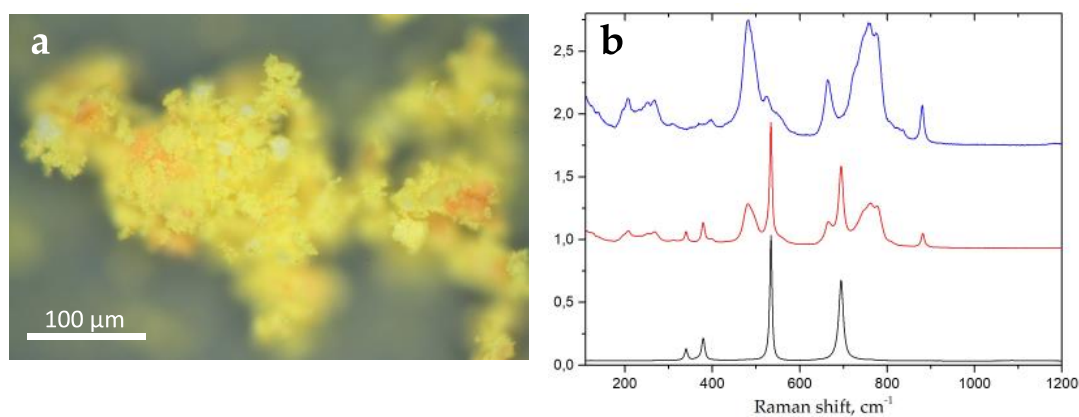


**Figure S8** (a) Optical image of  $\text{CaUO}_4$  powder. Yellow crystals are of  $\text{CaUO}_4$ , orange – of  $\text{CaU}_2\text{O}_7$  impurity; (b) Raman spectrum of  $\text{CaU}_2\text{O}_7$  (blue),  $\text{CaU}_2\text{O}_7$  impurity in  $\text{CaUO}_4$  (red),  $\text{CaUO}_4$  (black), recorded at 633 nm.

**Table S7** Raman shifts of Ca uranates compared to literature data for Ca and alkali-metal uranates. Ionic charges are omitted for simplicity.

Compound	CaUO <sub>4</sub>	CaUO <sub>4-x</sub>	Li <sub>2</sub> UO <sub>4</sub>	Na <sub>2</sub> UO <sub>4</sub>	K <sub>2</sub> UO <sub>4</sub>	Rb <sub>2</sub> UO <sub>4</sub>	Cs <sub>2</sub> UO <sub>4</sub>
			225, 248, 273, 280	238	221	230	238
	340	267	321, 350, 366	329, 362	293, 344		339, 369
	379	351	425, 446, 475, 491	442	439, 492	444	446
	534	533		506, 547			
	695	695	675, 710	712, 736	694	682	713,736
Compound	CaU <sub>2</sub> O <sub>7</sub>	CaU <sub>2</sub> O <sub>7</sub>	Li <sub>2</sub> U <sub>2</sub> O <sub>7</sub>	Na <sub>2</sub> U <sub>2</sub> O <sub>7</sub>	K <sub>2</sub> U <sub>2</sub> O <sub>7</sub>	Rb <sub>2</sub> U <sub>2</sub> O <sub>7</sub>	Cs <sub>2</sub> U <sub>2</sub> O <sub>7</sub>
	206, 251, 267			202, 233, 274	245, 267, 287	235, 247, 285	224, 258, 270, 292
	308, 369			313, 357	336	331	312, 340, 371
	398, 483		427	420	434, 491	442, 483	425, 474
	525			536	562	547	
	664		635	584, 599			
	725			752			713,736
	758, 780		765, 793	779, 788	778	778	778, 794
	881			826			818
Reference	This work	Allen & Griffiths (1979)		Volkovich et al. (1998)		Volkovich et al. (2001)	

## S4. XANES

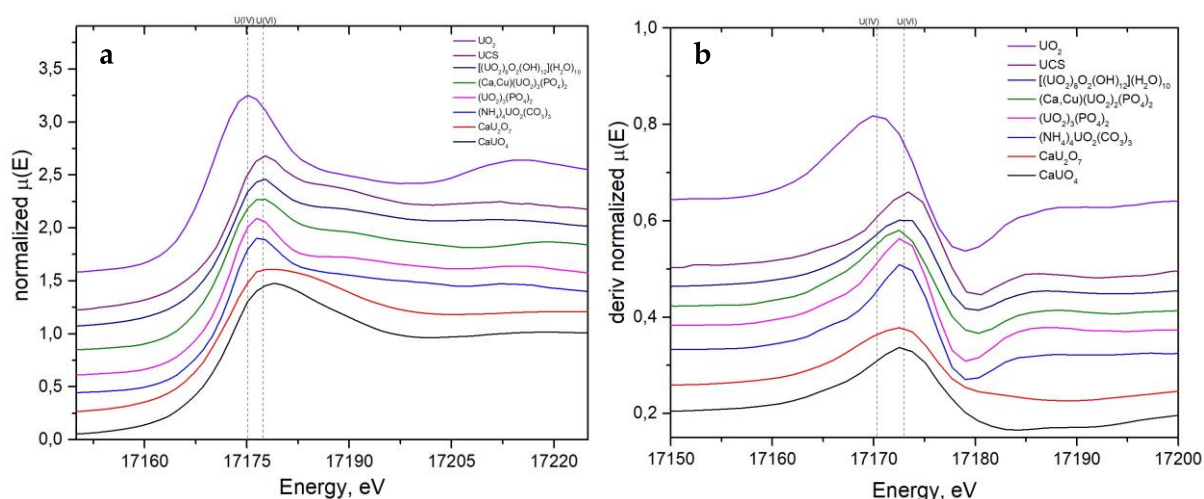


**Figure S9** (a) U L<sub>III</sub>-edge XANES spectra; (b) normalized derivatives of U L<sub>III</sub>-edge XANES spectra of studied compounds and references:  $\text{UO}_2$  ( $\text{U}^{4+}$ ), metaschoepite ( $\text{U}^{6+}$ ). XANES spectrum of UCS sample was presented and discussed in Maryakhin et al. (2021).

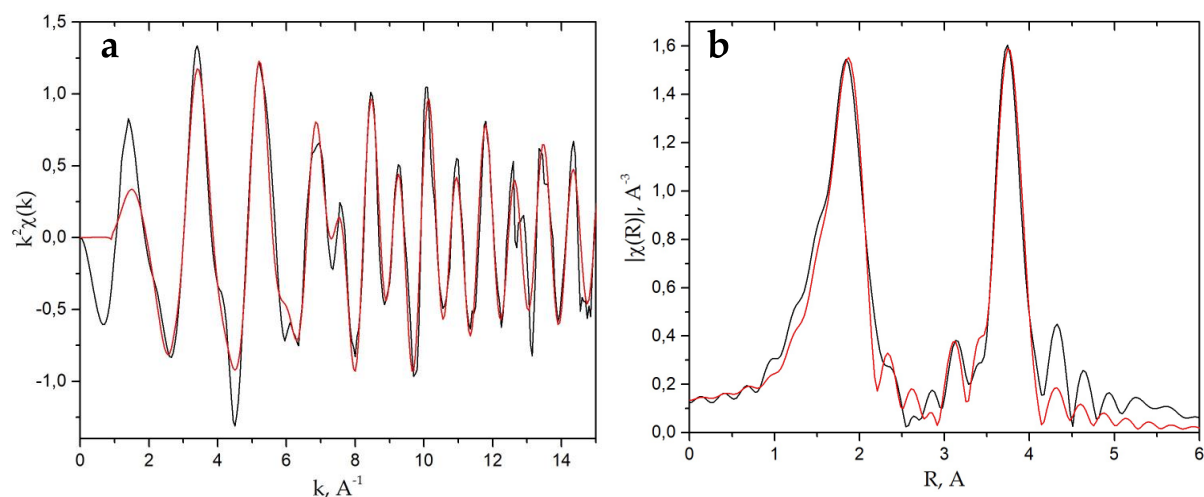


**Figure S10** (a) U L<sub>III</sub>-edge edge  $k^2$ -weighted EXAFS spectrum of  $\text{UO}_2$ ; (b) Fourier transform magnitude ( $k$  range 3-15), not corrected for phase shifts. Black lines are experimental data, red lines represent fit curves.

**Table S8** Fitting of UO<sub>2</sub> spectrum in comparison to literature data.

U-O (1)			U-U			U-O (2)			Reference
CN	R, Å	$\sigma^2, \text{Å}^2$	CN	R, Å	$\sigma^2, \text{Å}^2$	CN	R, Å	$\sigma^2, \text{Å}^2$	
8	2.37		12	3.86		24	4.53		Wasserstein (1951)
7.8±0.5	2.35±0.01	0.009	11.4±4	3.87±0.01	0.005	22.8±7.9	4.49±0.02	0.01	O'Loughlin et al. (2003)
8.1±2.4	2.34		6.3±1.9	3.86					Opel et al. (2007)
8	2.38	0.003	12	3.90	0.005				Denecke et al. (2005)
8	2.37±0.01	0.007	12	3.88±0.01	0.004	24	4.54±0.04	0.017	Boyanov et al. (2007)
8	2.34±0.01	0.012	6.2±0.8	3.85±0.02	0.007				Boyanov et al. (2017)
8	2.34	0.008	12	3.85	0.005	24	4.49	0.009	Jovani-Abril (2014)
8	2.34	0.004	12	3.87	0.004	24	4.52	0.008	This work

**S5. References**

- Allen, G.C.; Griffiths A.J. (1979). *J.C.S. Dalton*, **2**, 315–319.
- Armstrong, C.R. (2009). Publisher: Washington, USA. pp. 33–37.
- Boyanov, M.I.; Latta, D.E.; Scherer, M.M.; O'Loughlin, E.J.; Kemner, K.M. (2017). *Chem. Geology*, **464**, 110–117.
- Boyanov, M.I.; O'Loughlin, E.J.; Roden, E.E.; Fein, J.B.; Kemner, K.M. (2007). *Geochim. et Cosmochim. Acta*, **71**, 1898–1912.
- Denecke, M.A.; Janssens, K.; Proost, K.; Rothe, J.; Noseck, U. (2005). *Environ. Sci. Technol.*, **39**, 2049–2058.
- Faulques, E.; Perry, D.L.; Kalashnyk, N. (2018). *Vibrational spectroscopy*, **99**, 184–189.
- Frost R.L.; Carmody O.; Erickson, K.L.; Weier, M.L.; Cejka, J. (2004). *J. of Molecular Structure*, **703**, 47–54.
- Frost, R.L.; Weier, M. (2004). *Spectrochimica Acta Part A*, **60**, 2399–2409.

- Jovani-Abril, R. (2014). Doctoral thesis. Universidad de Santiago de Compostela (USC), Spain; Institute for Transuranium Elements (ITU), Germany.
- Maryakhin, M.A.; Vlasova, I.E.; Varlakova, G.A.; Germanov, A.V.; Varlakov, A.P.; Kalmykov, S.N.; Petrov, V.G.; Pomanchuk, A.Yu.; Yapaskurt, V.O.; Trigub, A.L. (2021). *Radiochemistry*, **63**, 119–126.
- O'Loughlin, E.J.; Kelly, S.D.; Cook, R.E.; Csencsits, R.; Kemner K.M. (2003). *Environ. Sci. Technol.*, **37**, 721–727.
- Opel, K.; Weiß, S.; Hübener, S.; Zänker, H.; Bernhard, G. (2007). *Radiochim. Acta*, **95**, 143–149.
- Pham-Thi, M.; Colomban, Ph. (1985). *J. of the Less-Common Metals*, **108**, 189–216.
- Volkovich, V.A.; Griffiths, T.R.; Fray, D.J.; Fields, M. (1998). *Vibrational Spectroscopy*, **17**, 83–91.
- Volkovich, V.A.; Griffiths, T.R.; Thied, R.C. (2001). *Vibrational Spectroscopy*, **25**, 223–230.
- Wasserstein, B. (1951). *Nature*, **168**, 380.